

1 Article

2 *VpStyA1* and *VpStyA2B* of *Variovorax paradoxus* 3 **EPS: Rather an Aryl Alkyl Sulfoxidase than a Styrene** 4 **Epoxidizing Monooxygenase**

5 Dirk Tischler^{1,2*}, Ringo Schwabe¹, Lucas Siegel¹, Kristin Joffroy¹, Stefan R. Kaschabek¹, Anika
6 Scholtissek¹ and Thomas Heine¹

7 ¹ Affiliation 1; Institute of Biosciences, Environmental Microbiology, TU Bergakademie Freiberg, Leipziger
8 Str. 29, 09599 Freiberg, Germany; dirk-tischler@email.de, ringoschwabe007@gmail.com,
9 lucasbenedikt@aol.com, kristin.friebel@student.tu-freiberg.de, stefan.kaschabek@ioez.tu-freiberg.de,
10 anika.scholtissek@gmail.com, heinet@tu-freiberg.de

11 ² Affiliation 2; Microbial Biotechnology, Ruhr University Bochum, Universitätsstr. 150, 44780 Bochum,
12 Germany

13 * Correspondence: dirk.tischler@rub.de; Tel.: +49-234-32-22656

14 **Abstract:** *VpStyA1* and *VpStyA2B* of *Variovorax paradoxus* EPS is annotated and characterized as the
15 first representative of an E2-type styrene monooxygenase of proteobacteria. It comprises a single
16 epoxidase (*VpStyA1*) and a fusion protein (*VpStyA2B*) which serves mainly as NADH:FAD-
17 oxidoreductase. *VpStyA2B* had a K_m of $33.6 \pm 4.0 \mu\text{M}$ for FAD and a k_{cat} of $22.3 \pm 1.1 \text{ s}^{-1}$. *VpStyA2B*
18 and *VpStyA1* showed monooxygenase activity on styrene of 0.14 U mg^{-1} and 0.46 U mg^{-1} as well as
19 on benzyl methyl sulfide of 1.62 U mg^{-1} and of 3.11 U mg^{-1} . A putative fusion region at position 408
20 (AREAV) was mutated to provide insights on *VpStyA2B*-function. The best mutant (408-AAAAA)
21 obtained showed a 6.6-times higher affinity for FAD while keeping the NADH-affinity and -
22 oxidation activity. Corresponding epoxidase activity increased (1.6-times). But, other mutants
23 showed still NADH:FAD-oxidoreductase activity, but lost mostly their epoxidase activity indicating
24 effects on the monooxygenase-part as well. Thus, this monooxygenase system represents an
25 interesting candidate for biocatalyst development.

26 **Keywords:** sulfoxidation; epoxidation; two-component monooxygenase; flavoprotein;
27 enantioselective biotransformation; fusion protein; protein linker; soil microorganism
28

29 1. Introduction

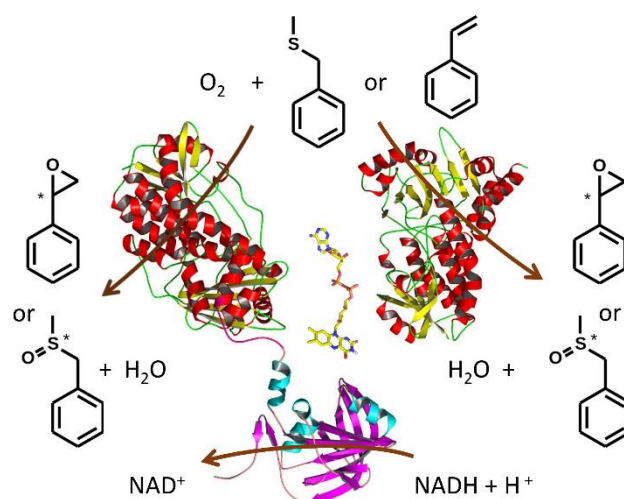
30 Flavin-dependent monooxygenases are able to catalyze a number of biotechnological important
31 reactions which are often regio- and enantioselective [1-3]. These enzymes can be divided into eight
32 groups according to their structure and function. For many purposes selective epoxidation and
33 sulfoxidation became attractive [4-11] and among those flavin-dependent styrene monooxygenases
34 (SMOs) exist as a group performing both reactions with a certain selectivity [2,5-10]. This is group E
35 among the flavin-dependent monooxygenases which can be described as follows (EC 1.14.14.11). It
36 is a two-component system at which a strictly NADH-dependent reductase (StyB; EC 1.5.1.36)
37 produces reduced FAD for the monooxygenase component (StyA, StyA1). Some of these reductases
38 occur as self-sufficient fusion proteins of an oxygenase and reductase domain (StyA2B) and those
39 represent the prototype of E2 like SMOs which was first described from a *Rhodococcus* [5]. Most of the
40 monooxygenases (StyA, StyA1) described so far utilize styrene as major substrate and belong even to
41 a natural styrene degradation pathway [11]. Recently, some E2-type SMOs have been discussed as
42 initial part of indole detoxification or degradation [12,13]. Thus they can also be described as indole
43 monooxygenases, IMOs.

44 SMOs rely on the flavin cofactor flavin adenine dinucleotide (FAD). The reduced flavin is
45 transferred by diffusion or by a direct transfer between both components [14-16]. The

46 monooxygenase tightly binds the reduced cofactor and the oxygen driven catalysis gets initiated [14-
 47 18]. Here oxygen gets activated by the reduced flavin to a (hydro)peroxy-FAD which can attack the
 48 actual substrate. Upon substrate oxygenation a hydroxyl-FAD intermediate is formed and
 49 decomposes to oxidized FAD and water [17-19]. The product is subsequently released and another
 50 catalytic cycle can start.

51 Styrene monooxygenases of type E2 have been shown to be excellent in sulfoxidation with
 52 respect to substrate conversion and enantioselectivity whereas the E1 type only shows a high activity
 53 at low enantioselectivity [1-10]. However, so far there is only a single E2 type SMO in detail studied
 54 and it has a comparable low activity [5,6,9]. Thus, it was reasonable to screen for further E2 type SMO
 55 candidates which can be applied in biocatalysis.

56 Powered by our former studies on E2 type SMOs [4-6,9,11,20,21] we took the chance to
 57 investigate the phylogenetic more distinct system *VpStyA1/VpStyA2B* of *Variovorax paradoxus* EPS
 58 (accession numbers: ADU39063 and ADU39062). Thus we here present its general activity, capability
 59 to act on styrene but also on sulfides (Scheme 1) compared to other monooxygenases and to evaluate
 60 its biotechnological applicability.
 61



62

63 **Scheme 1.** Cartoon of styrene monooxygenase activity. The reductase domain of StyA2B reduces FAD
 64 (displayed in oxidized form between protein monomers) upon NADH-consumption. Reduced FAD
 65 can be used by both monooxygenase units StyA1 (major; right) and StyA2 (minor; left) to activate
 66 molecular oxygen and to subsequently oxygenate the substrates (here for example styrene and benzyl
 67 methyl sulfide) [5-10]. Upon substrate oxygenation hydroxyl-FAD is formed and thereof water is
 68 eliminated to recycle the FAD in its oxidized form for the next catalytic cycle.

69 2. Results and Discussion

70 2.1. Evolution of *VpStyA1* and *VpStyA2B* from strain EPS

71 Already during an earlier study, the putative genes encoding for *VpStyA1* and *VpStyA2B* and
 72 thus the respective gene cluster of strain EPS had been identified [20]. According to a phylogenetic
 73 analysis and the surrounding genomic region the proteins were assigned as SMO related to the E2
 74 prototype of *Rhodococcus opacus* 1CP [5,6,11]. Interestingly, the sequence similarity of *VpStyA1* and
 75 *VpStyA2B* (74 % identity over 404 amino acids) between both monooxygenase subunits was much
 76 higher as among other StyA1/StyA2B couples. Further, they form together a separate branch in a
 77 distance tree of monooxygenase components [20,22]. As in the meanwhile more of those putative
 78 sequences had been released we could refine the phylogenetic study and try to understand the fusion
 79 event in more detail (Fig. 1). Respectively, the fusion event was discussed as functionally convergent
 80 event which is reinforced by the updated phylogenetic distance tree. However, no activity of these
 81 putative SMOs of type E2 originating of *Variovorax* species has been reported until now!

82

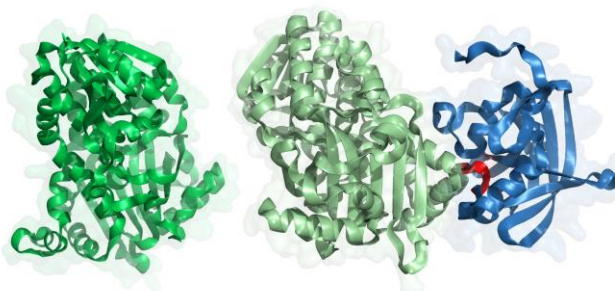
```

          385          405          425
Fusion proteins (StyA2B-like; E2-type)
ADU39062 : FDDRFAPWFDAAEADRFTEARAREAVV-----DR---FRRDPRKANGGE : 428
KIQ18477 : FDDRFVFPWFDAEADRFTEARAREAVV-----DR---FRRDPRKANGGE : 429
SDZ48663 : FDDRFIFFPWFDAEADRFTEARAREAVV-----DR---FRRDPRKANGGE : 428
SFQ22437 : FDDRFAPWFDAAEADRFTEKAREAAA-----DR---FRRDPRKANGGE : 428
ACR43974 : FDDRTVHNWFDAAEADRFENARAEAOQ-----FPRDLPRKANGGE : 426
ABM10099 : FDDRTSYFVWFDPTAAALFQARKEDDAAA-----FVRLPRKANGGE : 433
BAD56094 : FDDSTLHDWVFDGDAERWVAVRAAERS-----VPRALPRKANGGE : 421

Oxygenase components (StyA1-like; E2-type)
ADU39063 : FDDRTFFPWADAESERYTATCAAVA*----- : 412
ACR43973 : FDDRDFYHWMTPEAAQVITDVAN*----- : 406
ABM07034 : FDDRDFQWVMPDKAASVLDLSAAKVS*----- : 413
BAD56093 : FDDRDFHWVMDPDSAKSVLDDLAVAA*----- : 409

Regular two component systems (StyA/StyB-like; E1 and E2-type)
ABB03727/8 : FNYERQWDRSSPERIGQWCSQYAPTIAA*----MTLKKDVVVDIESTNFRCAVALF : 438
CAB06823/4 : FNYERQWDRSSPERIGQWCSQYAPTIAA*----MTLKKDVAVDIESTNFRCAVALF : 438
AAC23718/9 : FNYERQWDRSSPERIGQWCSQYAPTIAA*----MTLKKDMAVDIESTNFRCAVALF : 438
ABV24041/2 : FNYERHWDVSAASERIQAWERTAPAAPVRATA*----MQRAIPLAFRCAASRF : 432
ABQ12175/6 : FNYERPNFPWTDATACEAFIAAKSTRAAA*----MAALDWGSTDLHPKVIKGVVGSY : 436
ADE62390/1 : FNYERQWDRSSPERIGHWCSQYAPTIAA*----MTLKTDAAVETIASSFRCAVALF : 438

```



83

84

85

86

87

88

89

90

91

Figure 1. (Top) Sequence alignment of StyA2B-like proteins in comparison to functional StyA and StyB components. (Bottom) homology model of *VpStyA1* (darkgreen) *VpStyA2B* (monooxygenase – lightgreen, reductase – blue). The proposed linker region is illustrated in red. Numbering on top is according to *VpStyA2B* and the terminal amino acids are given at the end of lines. (*ADU_V. paradoxus* EPS; *KIQ_V. paradoxus* MEDvA23; *SDZ_Variovorax* sp. YR266; *SFQ_Variovorax* sp. OK605; *ACR_R. opacus* 1CP; *ABM_Paenarthrobacter aureescens* TC1; *BAD_Nocardia farcinica* IFM 10152; *ABB_Pseudomonas putida* SN1; *CAB_P. fluorescens* ST; *AAC_P. taiwanensis* VLB120; *ABV_uncultured* bacterium; *ABQ_uncultured* bacterium/MoxY; *ADE_Pseudomonas* sp. LQ26).

92

93

94

95

96

97

98

99

100

101

102

103

104

105

106

107

108

109

110

111

Mining the databases for *styA2B*-like genes/proteins revealed that they occur mainly among genera of Actinobacteria (e.g. *Amycolatopsis*, *Arthrobacter*, *Gordonia*, *Mycobacterium*, *Nocardia*, *Paenarthrobacter*, *Paeniglutamicibacter*, *Pseudarthrobacter*, *Sciscionella*, *Sinomonas*, *Streptomyces*, among others) but also among *Variovorax* (date of BLAST search: 19th Sep. 2017). So far there are no *styA2B*-like genes found in other none-Actinobacteria. However, there exist other *styA/styB* genes closely related to this subtype E2 of SMOs in various genera. The closest homologue to *Variovorax* SMOs are found in *Delftia* although no fusion variant is present. Already with the first report of *RoStyA2B* the linker region was recognized, but not investigated [5]. This we now did by mean of sequence alignments as well as molecular modelling (Fig. 1). And we identified a less conserved region/loop at the C-terminal site of the monooxygenase domain components of *StyA2B*-like proteins as potential linker region. In case of *VpStyA2B* it is located around region 408-AREAV-412. From the alignment of *StyA2B*-, *StyA1*- and *StyA*-like sequences it gets clear that the last conserved amino acid among those proteins is at position 404 (*VpStyA2B*) and in case of the none-fused proteins the following C-terminal parts are variable. In case of the fusion proteins next to this region the domain of the NADH:FAD oxidoreductase (B-part) is localized. There the first conserved amino acid is at position 417 (*VpStyA2B*) with respect to related *StyA2B*- and *StyB*-like proteins. This region from 404 to 417 represents a flexible loop between two helices according to the models obtained from homology modelling. This is not surprising as there is no sequence-structure relation available for this part. However, it fits to earlier made observations in which the start of the reductase domain was investigated [9,19,20,23]. Respectively, this proposed linker region need to be investigated.

112

113

114

Adjacent to the monooxygenase domain and the proposed linker region the reductase domain of the fusion proteins follows. Interestingly, the reductase sequence misses in all cases a few amino acids (range: 3 to 14) when compared to the *StyB* reductases of E1 type SMOs (Fig. 1) [5,7]. The

115 mentioned linker region was now target for a subsequent site-directed mutagenesis investigation. In
 116 all cases the original sequence (408-AREAV) was replaced or even extended. The following mutants
 117 have successfully been prepared and verified by sequencing: 408-TIVVVV, 408-AAAAA, 408-
 118 HHHHH, 408-WYHHH, 408-WYHHHHH, and 408-GQWCSQY. In order to validate the made
 119 assumptions, the wildtype protein *VpStyA2B* and the mutant proteins were produced and assayed.
 120 The chosen linker sequences of mutants to be produced base on the following rationale. Linker with
 121 A- and V-rich sequences were chosen to be flexible or H-rich to be more rigid. Whereas, the WY-H-
 122 variants should represent bulkier and thus even more restricted linkers. The 408-GQWCSQY motif
 123 represents a terminal part of a StyA-protein originating of pseudomonads (Fig. 1) and was picked as
 124 a comparison with respect to earlier made fusion proteins [19].

125 2.2. Molecular genetic work and enzyme production

126 The cloning of both genes, *VpstyA1* and *VpstyA2B*, as well as the generation of mutants was
 127 successfully accomplished which had been verified by sequencing the inserts of gene expression
 128 plasmids as described in experimental section (See supporting information, Table S1) and by a simple
 129 activity assay. Since *E. coli* BL21 derivatives allow the formation of indole from tryptophan during
 130 growth on complex medium as used herein, the activity of styrene monooxygenases and related
 131 enzymes can be verified by indole transformation to indigo [4-6,10,11,19]. And indeed, all clones
 132 obtained (*E. coli* BL21 (DE3) pLysS derivatives harboring the wildtype or mutant genes in a pET-
 133 vector) produced indigo during cultivation even without being induced for overexpression of target
 134 proteins. Clones which showed highest rate in indigo formation had been selected, propagated and
 135 stored as glycerol stocks for later protein production and characterization efforts.

136 Gene expression and protein purification was performed as described elsewhere [9]. The
 137 individual clones were cultivated either in a 3 L-fermenter or in 1 L-flasks in LB medium with
 138 appropriate antibiotics and 0.1 mM IPTG as inductor as described previously. In both cases (*VpStyA1*
 139 and *VpStyA2B*), enzyme production was successfully achieved with a yield of 2 to 4 mg_{*VpStyA2B*} and up
 140 to 9 mg_{*VpStyA1*} protein per liter broth, respectively. This is in congruence to other studies. Subsequently,
 141 the proteins produced and purified were characterized.

142 2.3. Reductase activity of *VpStyA2B* and mutants

143 The fusion protein *VpStyA2B* of strain EPS was supposed to be rather a reductase of the complete
 144 SMO system [6,7], and was for those reasons in analogy to the enzyme of strain 1CP characterized.

145 The protein *VpStyA2B* was successfully produced (verified by SDS-PAGE, not shown). The
 146 fraction obtained from Ni-chelate chromatography was slightly yellow which is an indicator for a
 147 bound flavin. This was analyzed as described for other SMOs and FAD was clearly determined by
 148 means of RP-HPLC as well as by spectroscopic methods and the use of authentic standards. A FAD
 149 saturation of 4.9 to 20.8 mol-% was calculated for the protein applied. This is in congruence to results
 150 obtained earlier for *RoStyA2B* [6,17]. This fraction was immediately assayed for activity and then
 151 concentrated and stored at -20 °C in a suitable storage buffer until characterization. Indeed, it could
 152 use NADH as source for reducing equivalents in order to reduce flavins. NADH cannot be replaced
 153 by NADPH. But, in case of the flavins FAD, FMN and riboflavin can be acceptors of reducing
 154 equivalents (Table 1). However, a clear preference could not be determined with respect to catalytic
 155 efficiency, which was for all here employed flavins between 0.57 and 0.88 s⁻¹ μM⁻¹, respectively.

156

157 **Table 1.** NADH:flavin oxidoreductase activity of *VpStyA2B* (MW = 66.32 kDa which was calculated
 158 from the amino acid sequence including the N-terminal tag).

Donor ¹ / Acceptor [μM] ²	K _m [μM]	V _{max} [U mg ⁻¹]	k _{cat} [s ⁻¹]	k _{cat} K _m ⁻¹ [s ⁻¹ μM ⁻¹]
---	------------------------	---	--	--

NADH (7.9 - 164) / FAD (70)	24.0 ± 4.0	16.2 ± 0.8	17.9 ± 0.9	0.72
NADH (164) / FAD (6.3 - 78.8)	33.6 ± 4.0	20.2 ± 1.0	22.3 ± 1.1	0.64
NADH (164) / FMN (4.1 - 90.2)	45.9 ± 6.8	26.0 ± 1.8	28.7 ± 1.9	0.57
NADH (164 μM) / Riboflavin (6.3 - 88.2)	37.7 ± 7.2	31.3 ± 2.7	34.6 ± 2.9	0.88

159 ¹ NADPH (230 μM in presence of 70 μM FAD) did not serve as an electron donor.

160 ² Either electron donor or acceptor was present in excess and the data obtained of triplicates were analyzed
161 assuming Michaelis-Menten kinetics.

162 The reductase activity and catalytic efficiency of *VpStyA2B* is up to 10-times higher than reported
163 for the *Rhodococcus* enzyme *RoStyA2B* [5]. Thus, differences on amino acid level (57 % identity) are
164 reflected within the biochemical properties of *StyA2B*-like SMOs. Still, the activity of the fusion
165 protein is by an order of magnitude lower if compared to most reductases of two-component systems
166 [22-24]. However, it was reported recently that the *N*-terminal fusion to the monooxygenase
167 drastically decreases the oxidoreductase activity in *RoStyA2B* [23]. In addition, an artificial fusion
168 protein was constructed from two-component relatives of *Pseudomonas* [19]. Herein, the coupling was
169 improved and the catalytic mechanism changed. It was also shown that the *N*-terminal region of the
170 reductase influences the binding and affinity for the substrate [19,22]. Therefore, it is likely that the
171 same is true for *VpStyA2B*. However, it is likely that this effect of the fusion to *StyA2* is different in
172 dependence of the linker region in the *Variovorax* enzyme.

173 In contrast to the monooxygenase part (*StyA2*), promiscuity towards the flavin cosubstrate is in
174 accordance with most characterized SMO reductases. And so far, only one representative from strain
175 1CP (*RoStyB*) is reported to be selective for FAD [9,22-24].

176 *VpStyA2B* was tested for inhibition or activation by a number of compounds used in other SMO
177 studies as well. Concentrations were adjusted to those of other studies or relevant for herein
178 performed enzyme assays. The NADH:FAD oxidoreductase test was employed. Therefore, the
179 enzyme was pre-incubated with a compound for 10 min at 20 °C. And the following relative activities
180 compared to the wildtype enzyme were determined (Fig. S1): a) No effect was observed for styrene
181 (2 mM), styrene oxide (100 μM), methyl phenyl sulfoxide (200 μM), H₂O₂ (100 μM), iodoacetamide (2
182 mM), sodium azide (500 μM) and Mg²⁺ (20 μM). b) A decrease in effect was determined in presence
183 of styrene oxide (200 μM; 87 % rel.-activity remained), methyl phenyl sulfide (2 mM; 24%), EDTA (1
184 mM; 88%), Fe²⁺ (100 μM; 74%), Fe³⁺ (100 μM; 65%), Ni²⁺ (100 μM; 81%), Zn²⁺ (100 μM; 35%), Ag⁺ (10
185 μM; 0%), Cd²⁺ (10 μM; 15%) and Hg⁺ (10 μM; 25%). c) And an increased activity was determined for
186 *o*-phenantroline (1 mM; 132%), DTT (500 μM; 186%), mercaptoethanol (500 μM; 166%), Ca²⁺ (100 μM;
187 198%) and Mn²⁺ (100 μM; 165%). The effects of the herein tested compounds are similar as observed
188 for *RoStyA2B* [5]. Thus it can be concluded, that there is no metal dependency present. Moreover, in
189 contrast to *RoStyA2B*, the activity is lowered by addition of Fe-ions, while Fe³⁺ has a stronger effect.
190 This is in accordance with inhibition studies on the reductase *StyB* from the two-component systems
191 of *Pseudomonas taiwanensis* VLB120 and *Acinetobacter baylyi* ADP1 [22,24]. Here, the effect of Fe²⁺ is
192 even stronger. However, reducing agents as DTT and divalent ions as Ca²⁺ support the performance
193 of *VpStyA2B*. This was also observed for *RoStyA2B* as well as *AbStyB* although the mechanism is
194 likely different. In contrast to *RoStyA2B*, *VpStyA2B* and *AbStyB* are insensitive against hydrogen
195 peroxide and the protective effect might therefore not be attribute towards oxidation of cysteine
196 residues. It was rather proposed to be a masking of Ni²⁺-ion that impeded the reductase [22].
197 However, this is unlikely as two additional purification steps were applied for the *VpStyA2B*
198 preparation and majority of the Ni²⁺ should be removed. Interestingly, thioanisole decreases the
199 reductase activity, which was not observed for SMO-reductases before.

200 In order to investigate the fusion region of this protein affords to determine the respective region
 201 had been accomplished on sequence level (see above) and served for the direction in a mutagenesis
 202 study. The six mutants of *VpStyA2B* obtained were separately produced and purified as described
 203 above and in analogy to the wildtype characterized for their NADH:FAD oxidoreductase activities
 204 (Table 2). During expression also these clones produced significant amounts of indigo indicating a
 205 functional expression of respective SMO-variants.

206 **Table 2.** NADH:flavin oxidoreductase activity of *VpStyA2B*-mutants and -wildtype.

<i>VpStyA2B</i> -variant	Donor NADH ¹		Acceptor FAD ¹	
	K_m [μM]	V_{max} [U mg ⁻¹]	K_m [μM]	V_{max} [U mg ⁻¹]
wildtype <i>VpStyA2B</i>	24.0	16.2	33.6	20.2
408-TIVVV	37.7	3.3	5.1	3.1
408-AAAAA	28.1	8.9	1.8	8.8
408-HHHHH	44.2	2.5	14.5	3.1
408-WYHHH	20.1	7	3.2	6.9
408-WYHHHHH	40.6	13.8	7.4	13.2
408-GQWCSQY	47.6	3.8	14.5	3.7

207 ¹ Concentrations of NADH and FAD in order to determine kinetic properties were chosen as for the
 208 wildtype *VpStyA2B* given in Table 1. As previously triplicates were used to get the values and standard
 209 deviations were in all cases less than 15 % and thus comparable to Table 1.

210 The mutants were all active and it was possible to determine kinetic parameters as for the
 211 wildtype oxidoreductase. Respectively, the wildtype was most active with NADH and all the
 212 mutants showed a lower activity. However, the affinity for NADH seemed not to be altered as the
 213 K_m values were all in the same high range. This picture changed somewhat for the series collected for
 214 FAD. The general activities were similar to those for NADH-variation and also the order from the
 215 most active to the worst representative were same. But, the affinity for FAD was drastically different
 216 among the variants which was obvious from the K_m values determined. Thus, the best and most
 217 efficient variant was 408-AAAAA with respect to its oxidoreductase activity. Respectively, the
 218 catalytic efficiency of FAD-reduction is about $5.4 \text{ s}^{-1} \mu\text{M}^{-1}$ which is about 8.4-times more efficient than
 219 the wildtype. This is due to the tighter FAD binding expressed by the 6.6-times lower K_m value for
 220 FAD. Thus means the proposed linker region, which was mutated, has a strong effect on the FAD
 221 binding and turnover. This is in congruence to earlier studies which could demonstrate that the *N*-
 222 terminal part of NAD(P)H:flavin oxidoreductases is important for the flavin binding and thus for
 223 catalysis [19,23]. Further, it indicates that the selected region indeed can be the linker as it is functional
 224 relevant for the reductase domain.

225 2.4. Monooxygenase activity of *VpStyA1*, *VpStyA2B* and *VpStyA2B*-mutants

226 Already during the gene cloning and expression experiments the formation of indigo was
 227 observed and used to identify best protein producers as mentioned above. This was later verified by
 228 a plate assay as described in experimental section in order to get a view on the strains producing
 229 either a highly active SMO or a lot of this SMO (Table 3). The wildtype proteins *VpStyA1* and
 230 *VpStyA2B* and especially the mutant 408-AAAAA produced most indigo. The acceptance of indole
 231 as a substrate and the formation of indigo fits to a very recent finding that related E2 type
 232 monooxygenases were assigned to indole degradation and act basically as indole monooxygenases
 233 (IMOs) [12,13].

234 **Table 3.** Epoxidase activity of *VpStyA2B*-mutants and -wildtype enzymes.

Substrate	Styrene V_{\max} [mU mg ⁻¹]			Indole plate screening ⁴
	-	ETY ² [%]	extra RoStyBart ³	
SMO ¹	-	ETY ² [%]	extra RoStyBart ³	plate screening ⁴
wildtype <i>VpStyA1</i>	n.a.	n.a.	460	+++
wildtype <i>VpStyA2B</i>	159	1	140	++
408-TIVVV	135	4.4	327	+
408-AAAAA	260	3	260	+++
408-HHHHH	< 1	< 1	4	+
408-WYHHH	1.7	< 1	7.3	+
408-WYHHHHH	< 1	< 1	1.6	+
408-GQWCSQY	< 1	< 1	3.1	+

235 ¹ Mutants are made of *VpStyA2B* as described in methods and were in analogy to the wildtype investigated.

236 ² The electron transfer yield (ETY) was calculated from the NADH-consumption vs. epoxidation rate.

237 ³ In case of *StyA1* an additional NADH:FAD oxidoreductase was needed which could also assist *StyA2B*-
238 like proteins [6,23].

239 ⁴ The plate screening was performed with clones expressing respective genes on an agar plate and the
240 indigo formation was followed online by a camera.

241 n.a. = no activity measureable

242 The wildtype monooxygenases *VpStyA1* and *VpStyA2B* show a comparable epoxidase activity
243 as other SMOs (range 0.02 to 2.1 U mg⁻¹) (Table 3) [5-10,24]. *VpStyA1* is about 2.9-times and 2.1-times
244 more active than *VpStyA2B* and the *Rhodococcus* counterpart *RoStyA1*, respectively. And it was
245 confirmed that *VpStyA1* represents the major monooxygenase activity of the system as it was found
246 for the prototype *RoStyA1/RoStyA2B* [6]. This was expected but also indicates that the high sequence
247 similarity of the *Variovorax* monooxygenases does not change the catalytic properties to a large extent.
248 However, it is interesting that *VpStyA2B* is about 8.4-times more active on styrene as *RoStyA2B*. The
249 latter one could be boosted by additional FAD-reductase, but, *VpStyA2B* not. Later another batch of
250 *VpStyA2B* was produced for biotransformations. It showed only a specific epoxidase activity of 27
251 mU mg⁻¹ which is about 6-times lower. In this case surplus of reductase activity by an additional
252 FAD-reductase could boost the activity 2.3-times. This indicates that *VpStyA2B* can be saturated by
253 reduced FAD to a certain maximum as it was found for the *Rhodococcus* counterpart [6]. Another
254 difference between both *StyA2B*-proteins is the FAD-reductive power which is about 4.3-times higher
255 in case of *VpStyA2B* with a k_{cat} of 22.3 s⁻¹ vs. that of *RoStyA2B* of 5.2 s⁻¹. This might be the reason that
256 *VpStyA2B* can reach a maximum epoxidase activity even without an additional FAD-reductase (Table
257 1). Furthermore, the quality of the protein batches prepared can differ with respect to FAD saturation
258 as well as activity which is known for related enzymes [5,6,9,17]. However, we could not identify the
259 fact which led to this different specific activity as the only differences during enzyme production
260 were the fermentation volume and a final polishing step (gel filtration). The protein batches had
261 otherwise a similar concentration and purity after purification which was also consistent except for
262 the volumes applied. This needs further investigation.

263 The mutants obtained were in analogy to the wildtype enzymes characterized for their capability
264 to convert styrene into styrene oxide. The wildtype *VpStyA2B* showed an activity of 159 mU mg⁻¹.
265 The *VpStyA2B*-variants were prepared similarly and assayed immediately in order to allow a direct
266 comparison. The following relative styrene epoxidase activities were determined: 84.9 % for 408-
267 TIVVV, 163.5 % for 408-AAAAA and less than 2 % in case of the other variants (408-HHHHH, 408-

268 WYHHH, 408-WYHHHHH, and 408-GQWCSQY). This clearly indicates the region mutated has
 269 significant effects also on the epoxidase activity of StyA2B-proteins even if it seemed to be only the
 270 C-terminal part of the respective monooxygenase domain. Further, from the nature of this proposed
 271 linker sequence it can be reasoned that smaller hydrophobic residues yield higher activities compared
 272 to larger or more polar residues. This is indeed true for the FAD-reductase as well as the
 273 corresponding styrene epoxidase activity. And again the mutant 408-AAAAA showed a very
 274 promising catalytic behavior which was better than the wildtype in terms of activity and efficiency
 275 (Table 3). It was followed by variant 408-TIVVV which was even more active with surplus of reduced
 276 FAD formed by an additional FAD-reductase. It achieved almost the epoxidase activity of *VpStyA1*.
 277 This might allow to draw some conclusions as it might be possible to generate more efficient and
 278 catalytic active self-sufficient fusion proteins; here SMO-like proteins. But, as the mutagenesis of the
 279 C-terminal part of the StyA2-part improved catalytic properties it might be also possible to alter
 280 StyA1- or StyA-like proteins at their C-terminus in order to improve their catalytic behavior.
 281 However, structural investigations become necessary in order to elucidate the nature of substrate and
 282 cofactor binding to really understand why the mutants show a distinct activity and efficiency!

283 2.5. Biotransformation of sulfides

284 For the biotransformation experiments, another fresh batch of each enzyme (*VpStyA1* and
 285 *VpStyA2B*) was produced and the initial specific activity of styrene epoxidation was determined to
 286 27 mU mg⁻¹ *VpStyA2B*, 63 mU mg⁻¹ *VpStyA2B* and surplus *RoStyBart* as well as 121 mU mg⁻¹ *VpStyA1*
 287 and surplus *RoStyBart*, respectively [23]. The lower specific activities of these batches might be due
 288 to remaining impurities in the protein preparation as for these experiments after the Ni-chelate
 289 chromatography the additional gel filtration was omitted. Another important point is that the
 290 addition of extra reducing power in form of *RoStyBart* supports the monooxygenase performance, as
 291 it was discussed above and which is in congruence with earlier studies. For comparison, in the 2 h
 292 biotransformation assay with styrene as substrate, observed activities with surplus *RoStyBart* were
 293 0.002 U mg⁻¹ for *VpStyA2B* and 0.029 U mg⁻¹ for *VpStyA1*.

294 As target compounds sulfoxides had been chosen and thus kinetics and later on
 295 biotransformations were done with selected model sulfides. Kinetic parameters were determined as
 296 described above for styrene in order to allow a comparison. Maximum activity on the substrate
 297 benzyl methyl sulfide (BMS) from such kinetic studies was determined to 3.113 U mg⁻¹ *VpStyA1* and
 298 1.616 U mg⁻¹ *VpStyA2B*. This is about 25 to 26-times faster as the conversion of styrene. And taking
 299 the maximal epoxidase activity of *VpStyA1* (Table 3) into account, a specific activity of about 10 U
 300 mg⁻¹ could be possible. This high sulfoxidase activity of the SMO system of *Variovorax paradoxus* EPS
 301 is impressive and thus more sulfides were tested in a series of 2 h biotransformations (Table 4).

302 *VpStyA1* reaches observed activities of up to 0.281 U mg⁻¹ and BMS is the best substrate. These
 303 activities are much higher if compared to styrene as substrate. *VpStyA1* produces almost exclusively
 304 the (*S*)-sulfoxide products. *VpStyA2B* has lost about 97 % of its initial activity by up to 0.044 U mg⁻¹,
 305 but also preferably produces the (*S*)-enantiomer. However, due to the mentioned loss of activity the
 306 exact ee-determination failed.

307 However, both monooxygenases lost at least one order of magnitude of activity and it has to be
 308 elucidated what causes the decrease. It might be possible that there is product inhibition or that the
 309 enzymes are not stable over time under the assay conditions. Especially, the more complex fusion
 310 protein seems to be less stable in cell-free approaches.

311

312 **Table 4.** 2 h Biotransformation of sulfides. Activities are given in U mg⁻¹ and represent the observed
 313 activities determined after 2 h (no initial rates). Conversions of 2 mM substrate are given.

Substrate	Product	<i>VpStyA1</i> [U mg ⁻¹]	ee [%]	<i>VpStyA2B</i> [U mg ⁻¹]	ee [%]
-----------	---------	---	-----------	--	-----------

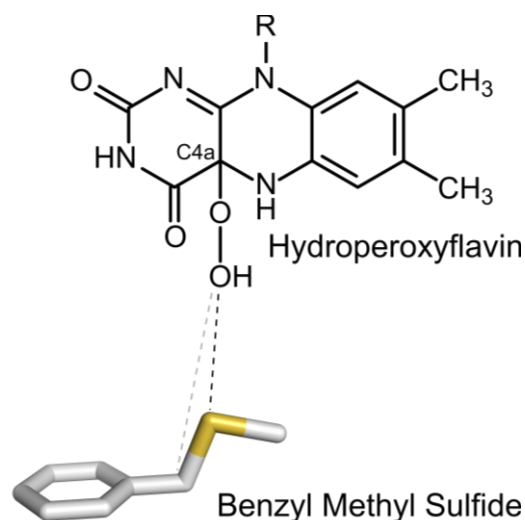
		(conversion [%])		(conversion [%])	
PMS		0.129 (43.6 ± 1.9)	98 (S)	0.021 (6.3 ± 0.3)	64 (S)
4F-PMS		0.177 (59.8 ± 0.4)	99 (S)	0.015 (4.3 ± 0.7)	84 (S)
4Cl-PMS		0.114 (38.5 ± 1.7)	99 (S)	0.015 (4.4 ± 0.4)	96 (S)
4Br-PMS		0.096 (32.4 ± 4.7)	99 (S)	0.021 (6 ± 0.7)	96 (S)
BMS		0.281 (95 ± 0.5)	97 (S)	0.044 (13 ± 0.9)	n.d. (S)

314 phenyl methyl sulfide (PMS), 4-fluoro phenyl methyl sulfide (4F-PMS), 4-chloro phenyl methyl sulfide
315 (4Cl-PMS), 4-bromo phenyl methyl sulfide (4Br-PMS), benzyl methyl sulfide (BMS); n.d. = not detectable

316 Also it need to be mentioned that in all cases no other products had been observed which could
317 indicate any overoxidation of sulfoxides to sulfones. This is an important feature to produce chiral
318 sulfoxides.

319 When comparing the sulfide biotransformations it gets obvious that they are for each enzyme in
320 the same order of magnitude. And in both cases a significant preference for the substrate benzyl
321 methyl sulfide was observed. Here the S-atom is one position more far from the aryl system as in case
322 of the other sulfides applied. This indicates that the activated oxygen of the hydroperoxy-FAD
323 intermediate in the active site of the monooxygenase is more closely located to this position of the
324 substrate and allows a faster attack (Scheme 2) [17,18]. This hypothesis needs to be verified by
325 structural and kinetic investigations. But, so far there is no experimentally proven SMO structure
326 inclusive substrate and cofactor available.

327



328

329

330

Scheme 2. Illustration of the putative binding and positioning of benzyl methyl sulfide towards the hydroperoxyflavin in the active site of SMOs from *V. paradoxus* EPS. Kinetic data indicate that the

331 distal position of the S-atom is likely closer to the C4a-hydroperoxyflavin, as BMS is preferred over
332 sulfides, were the S-atom is adjacent to the aryl group.

333 3. Materials and Methods

334 3.1. Synthesis of sulfoxides

335 Commercial sulfides served as base to produce sulfoxides which had been applied as standards
336 for analytical methods. The chemical sulfoxidation was achieved according to the protocol published
337 earlier [25] as it provided high yields of desired products. First a solution of 7 mmol sulfide in 100 ml
338 methanol and 20 ml water plus 10 ml titanium (III) chloride (16 % aqueous solution) was prepared.
339 Then dropwise a hydrogen peroxide solution (3.2 ml 30 % aqueous in 15 ml methanol) was added
340 while constantly stirring at ambient temperature (about 20 °C). Latest after 25 min the substrate was
341 completely converted and the reaction had been stopped by adding 50 ml water. Sulfoxides formed
342 had been extracted by chloroform (three times) and subsequently dried over anhydrous magnesium
343 sulfate. Chloroform was further removed under reduced pressure. Success of reactions and purities
344 of products had been determined as described elsewhere [26].

345 3.2. Nucleotides, sequence analysis and molecular modelling

346 Sequence analyses based on a previously performed investigation [5]. Thus accession numbers
347 of the E2-type SMO components originating of *Variovorax paradoxus* EPS were already available:
348 ADU39063 (*VpStyA1*) and ADU39062 (*VpStyA2B*). These were used for a BLASTP search in order to
349 identify related or even homolog proteins. This allowed to generate an amino acid sequence
350 alignment in analogy to earlier reports [5,20]. This served as a template for the subsequent calculation
351 of a dendrogram and the modelling. As templates for homology modelling the two available
352 structures (PDB StyA: 3IHM, and PDB PheA2: 1RZ0) were employed [18,27]. The C-terminal StyA2-
353 part was linked to the N-terminal StyB-part by a random loop which gets obvious from Scheme 1 and
354 Figure 1, respectively. As tools have been employed: MEGA7 for the alignment, Modeller program
355 version 9.19 for the comparative homology modelling as well as GenDoc and PyMol V1.1r1 for
356 alignment and 3D-structure visualization [9,28-30].

357 3.3. Bacterial strains and cultivation

358 *Escherichia coli* strains DH5 α and BL21 (DE3) pLysS were cultivated for cloning and expression
359 as described elsewhere [5,6,9,31]. A list of genes, primers and plasmids for this work is presented in
360 the Supplemental Information (Table S1).

361 Indigo formation was observed during the cultivation and gene expression experiments. A plate
362 screening in order to monitor indigo formation was set up as follows. The expression clones were
363 transferred on a M9 mineral media agar-plate in a predefined grid, followed by a 22 h incubation at
364 30 °C [32]. The solid media was supplemented with antibiotics as described previously and 0.5 mM
365 isopropyl- β -D-thiogalactopyranosid for induction of protein expression [5,6,9,31]. Indigo formation
366 was started by spraying the plates with an indole-substrate solution (5 Mm Tris-HCl, pH 7.5, 50 mM
367 indole, 20 % DMSO). The plates were then transferred onto a white light-table in a darkened box
368 equipped with a camera. Pictures of the plates were shot in a 30 s interval. The color formation of
369 each colony was monitored and normalized upon colony size to get a time-resolved intensity profile
370 for each clone.

371 3.4. Molecular genetic work

372 The DNA sequences of *VpstyA1* (Accession number: MF781076) and *VpstyA2B* (MF781075) were
373 optimized for the codon usage and GC content of *Acinetobacter baylyi* ADP1 as described previously
374 [9,33]. The genes were purchased in a pEX-A vector system from Eurofins MWG (Ebersberg) with 5'-
375 NdeI and 3'-NotI restriction sites allowing for subcloning into pET16bP [9]. Site-directed mutagenesis
376 of the linker area was done by using the GeneMorph II EZClone Domain Mutagenesis Kit (Agilent

377 Technologies). Therefore, a megaprimer was generated by amplifying the target region with a primer
378 that contains the desired mutation. This megaprimer was annealed to the parental plasmid and
379 extended in the EZClone reaction. Then, the parental DNA was DpnI digested and the remaining
380 pET16bP construct harboring the mutation was transformed into *E. coli* BL21 cells for gene
381 expression. Successful mutation of the target genes was proven by sequencing of the plasmid using
382 the pET16-check-fw/pET16-check-rev primer [34].

383 3.5. Protein purification and quantification

384 Recombinant protein production and purification was done as described previously [9,23].

385 Protein concentration was determined by means of the Bradford method employing bovine
386 serum albumin as a standard [35]. The purity of protein preparations was controlled by SDS-PAGE
387 as described earlier for those types of proteins [5,6].

388 Further, the FAD content of proteins was determined by the protocol employed for *RoStyA1* and
389 *RoStyA2B* [6]. Therefore, authentic standards for FMN and FAD had been determined by RP-HPLC
390 connected to a diode array detector for UV/Vis range.

391 3.6. Enzyme assays and product analysis

392 Flavin oxidoreductase activity was determined spectrophotometrically (Cary 50, Varian) by
393 quantifying NAD(P)H consumption at 340 nm ($\epsilon_{340} \text{ nm} = 6.22 \text{ mM}^{-1} \text{ cm}^{-1}$). One unit of enzyme activity
394 is defined as the amount required to oxidize 1 μmol of NAD(P)H per min. All measurements were
395 carried out in triplicate. The standard assay (1 mL) consisted of 20 mM Tris-HCl, pH 7.5, 68 μM flavin
396 co-substrate (FAD, FMN or riboflavin) and 177 μM NADH. After incubating the mixture for 10 min
397 at 30 °C, the reaction was started by adding an appropriate amount of enzyme. For estimating steady-
398 state kinetic parameters, initial reaction rates were determined using 4.1 to 90.2 μM FAD and 7.9 to
399 164 μM NADH. Kinetic parameters were obtained by nonlinear regression analysis applying
400 KaleidaGraph 4.5 (Synergy Software), assuming Michaelis-Menten kinetics.

401 Monooxygenase activity assay and standard HPLC analytic were performed as described
402 previously [5,9]. Reduced FAD was supplied by an additional reductase *RoStyBart* [23] or 10 mM
403 BNAH, respectively.

404 The 2h biotransformations were done according to the standard monooxygenase assay by
405 adding the respective sulfides instead of styrene as substrate. Enantiomeric excess of obtained
406 products were analyzed as described previously for epoxides [5] and sulfoxides [26].

407 4. Conclusions

408 The styrene monooxygenase *VpStyA1* and *VpStyA2B* originating of *Variovorax paradoxus* EPS
409 was herein described as the first proteobacterial E2 type representative which also employs a fusion
410 protein as an NADH:FAD-oxidoreductase. Both proteins were successfully produced by recombinant
411 expression. The enzyme converts styrene in an enantioselective manner as well as a number of aryl
412 alkyl sulfides. However, it was by far more active (3.3 to 22-times) on these sulfides as on styrene.
413 Therefore, this enzyme can be proposed as an enantioselective sulfoxidase. Furthermore, the
414 potential fusion region of *StyA2B*-like proteins was identified and mutated. It was demonstrated that
415 this region has effects on the reductase as well as monooxygenase domain, and it is especially critical
416 for the FAD binding, probably of both domains. Structural and kinetic studies may reveal the effect
417 of the fusion on the individual domains of *VpStyA2B* and related monooxygenase. Thus, this SMO of
418 strain EPS is a suitable candidate for structural investigations as well as to develop an enantioselective
419 catalyst for sulfoxidation reactions.

420 **Supplementary Materials:** The following are available online at www.mdpi.com/link, Figure S1: Sensitivity of
421 *VpStyA2B* towards putative inhibitors determined by applying the NADH:FAD oxidoreductase assay, Table S1:
422 Strains, plasmids and primers used in this study.

423 **Acknowledgments:** We thank the DECHEMA for support by means of a Max-Buchner-Research Fellowship to
424 Dr. Dirk Tischler (MBFSt 3339) and the Saxon Government for funding (SAB 100263733). We appreciate the

425 support and valuable discussions by R. Weiße and N. Sträter (University of Leipzig) during drafting the
426 manuscript! Support for the open access submission was obtained from the Ruhr University Bochum.

427 **Author Contributions:** D.T. and T.H. conceived and designed the experiments; R.S. performed the mutagenesis
428 and analyzed mutants with respect to sequence and activity. S.R.K. performed the synthesis of sulfoxides and
429 contributed to the analysis; R.S., A.S., L.S., K.J. produced and analyzed the proteins, conducted the
430 biotransformations and analyzed the data; D.T. and T.H. wrote the paper. All authors approved the final version
431 of the manuscript.

432 **Conflicts of Interest:** The authors declare no conflict of interest. The founding sponsors had no role in the design
433 of the study; in the collection, analyses, or interpretation of data; in the writing of the manuscript, and in the
434 decision to publish the results.

435 References

- 436 1. Huijbers, M.M.E.; Montersino, S.; Westphal, A.H.; Tischler, D.; van Berkel, W.J.H. Flavin dependent
437 monooxygenases. *Arch. Biochem. Biophys.* **2014**, *544*, 2-17, DOI: 10.1016/j.abb.2013.12.005.
- 438 2. Montersino, S.; Tischler, D.; Gassner, G.T.; van Berkel, W.J.H. Catalytic and structural features of
439 flavoprotein hydroxylases and epoxidases. *Adv. Synth. Catal.* **2011**, *353*, 2301-2319, DOI:
440 10.1002/adsc.201100384.
- 441 3. van Berkel, W.J.H.; Kamerbeek, N.M.; Fraaije, M.W. Flavoprotein monooxygenases, a diverse class of
442 oxidative biocatalysts. *J. Biotechnol.* **2006**, *124*, 670-689, DOI: 10.1016/j.jbiotec.2006.03.044.
- 443 4. Tischler, D.; Kaschabek S.R. Microbial Styrene Degradation: From Basics to Biotechnology. In *Microbial*
444 *Degradation of Xenobiotics*, Singh, S.N., Eds.; Springer: Berlin Heidelberg, Germany, 2012; pp. 67-99, eISBN
445 978-3-642-23789-8.
- 446 5. Tischler, D.; Eulberg, D.; Lakner, S.; Kaschabek, S.R.; van Berkel, W.J.H.; Schlömann, M. Identification of a
447 novel self-sufficient styrene monooxygenase from *Rhodococcus opacus* 1CP. *J. Bacteriol.* **2009**, *191*, 4996-5009,
448 DOI: 10.1128/JB.00307-09.
- 449 6. Tischler, D.; Kermer, R.; Gröning, J.A.D.; Kaschabek, S.R.; van Berkel, W.J.H.; Schlömann, M. StyA1 and
450 StyA2B from *Rhodococcus opacus* 1CP: A multifunctional styrene monooxygenase system. *J. Bacteriol.* **2010**,
451 *192*, 5220-5227, DOI: 10.1128/JB.00723-10.
- 452 7. Toda, H.; Imae, R.; Komio, T.; Itoh, N. Expression and characterization of styrene monooxygenases of
453 *Rhodococcus* sp. ST-5 and ST-10 for synthesizing enantiopure (S)-epoxides. *Appl. Microbiol. Biotechnol.* **2012**,
454 *96*, 407-418, DOI: 10.1007/s00253-011-3849-3.
- 455 8. Hollmann, F.; Lin, P.-C.; Witholt, B.; Schmid, A. Stereospecific biocatalytic epoxidation: The first example
456 of direct regeneration of a FAD-dependent monooxygenase for catalysis. *J. Am. Chem. Soc.* **2003**, *125*, 8209-
457 8217, DOI: 10.1021/ja034119u.
- 458 9. Riedel, A.; Heine, T.; Westphal, A.H.; Conrad, C.; Rathsack, P.; van Berkel, W.J.H.; Tischler, D. Catalytic
459 and hydrodynamic properties of styrene monooxygenases from *Rhodococcus opacus* 1CP are modulated by
460 cofactor binding. *AMB Express* **2015**, *5*, 30, DOI: 10.1186/s13568-015-0112-9.
- 461 10. van Hellemond, E.W.; Janssen, D.B.; Fraaije, M.W. Discovery of a novel styrene monooxygenase originating
462 from the metagenome. *Appl. Environ. Microbiol.* **2007**, *73*, 5832-5839, DOI: 10.1128/AEM.02708-06.
- 463 11. Tischler D. Pathways for the degradation of styrene. In *Microbial Styrene Degradation*, Vol. 1, In
464 SpringerBriefs in Microbiology, Springer Int. Publishing, Germany, 2015; pp. 7-22, eISBN 978-3-319-24862-
465 2.
- 466 12. Lin, G.-H.; Chen, H.-P.; Shu, H.-Y.; Lee, S.-W. Detoxification of indole by an indole-induced flavoprotein
467 oxygenase from *Acinetobacter baumannii*. *PLoS ONE* **2015**, *10*, e0138798, DOI: 10.1371/journal.pone.0138798.
- 468 13. Sadauskas, M.; Vaitekūnas, J.; Gasparavičiūtė, R.; Meškys, R. Indole biodegradation in *Acinetobacter* sp.
469 strain O153: Genetic and biochemical characterization. *Appl. Environ. Microbiol.* **2017**, *83*, e01453-17, DOI:
470 10.1128/AEM.01453-17.
- 471 14. Kantz, A.; Chin, F.; Nallamotheu, N.; Nguyen, T.; Gassner, G.T. Mechanism of flavin transfer and oxygen
472 activation by the two-component flavoenzyme styrene monooxygenase. *Arch. Biochem. Biophys.* **2005**, *442*,
473 102-116, DOI: 10.1016/j.abb.2005.07.020.
- 474 15. Kantz, A.; Gassner, G.T. Nature of the reaction intermediates in the flavin adenine dinucleotide-dependent
475 epoxidation mechanism of styrene monooxygenase. *Biochemistry* **2011**, *50*, 523-532, DOI: 10.1021/bi101328r.

- 476 16. Morrison, E.; Kantz, A.; Gassner, G.T.; Sazinsky, M.H. Structure and mechanism of styrene monooxygenase
477 reductase: New insight into the FAD-transfer reaction. *Biochemistry* **2013**, *52*, 6063-6075, DOI:
478 10.1021/bi400763h.
- 479 17. Tischler, D.; Schlömann, M.; van Berkel, W.J.H.; Gassner, G.T. FAD C(4a)-hydroxide stabilized in a naturally
480 fused styrene monooxygenase. *FEBS Lett.* **2013**, *587*, 3848-3852, DOI: 10.1016/j.febslet.2013.10.013.
- 481 18. Ukaegbu, U.E.; Kantz, A.; Beaton, M.; Gassner, G.T.; Rosenzweig, A.C. Structure and ligand binding
482 properties of the epoxidase component of styrene monooxygenase. *Biochemistry* **2010**, *49*, 1678-1688, DOI:
483 doi: 10.1021/bi901693u.
- 484 19. Heine, T.; Tucker, K.; Okonkwo, N.; Assefa, B.; Conrad, C.; Scholtissek, A.; Schlömann, M.; Gassner, G.T.;
485 Tischler, D. Engineering styrene monooxygenase for biocatalysis: Reductase-epoxidase fusion proteins.
486 *Appl. Biochem. Biotechnol.* **2017**, *181*, 1590-1610, DOI: 10.1007/s12010-016-2304-4.
- 487 20. Tischler, D.; Gröning, J.A.D.; Kaschabek, S.R.; Schlömann, M. One-component styrene monooxygenases:
488 An evolutionary view on a rare class of flavoproteins. *Appl. Biochem. Biotechnol.* **2012**, *167*, 931-944, DOI:
489 10.1007/s12010-012-9659-y.
- 490 21. Tischler, D.; Riedel, A.; Schwabe, R.; Siegel, L.; Friebel, K.; Heine, T.; Gröning, J.A.D.; Kaschabek, S.R.;
491 Schlömann, M. Evolution der Styrol-Monooxygenase StyA1/StyA2B aus *Variovorax paradoxus* EPS und seine
492 biotechnologische Anwendung. *Chem. Ing. Tech.* **2014**, *86*, 1401-1426, DOI: 0.1002/cite.201450048.
- 493 22. Gröning, J.A.D.; Kaschabek, S.R.; Schlömann, M.; Tischler, D. A mechanistic study on SMOB-ADP1: an
494 NADH:flavin oxidoreductase of the two-component styrene monooxygenase of *Acinetobacter baylyi* ADP1.
495 *Arch. Microbiol.* **2014**, *196*, 829-845, DOI: 10.1007/s00203-014-1022-y.
- 496 23. Heine, T.; Scholtissek, A.; Westphal, A.H.; van Berkel, W.J.H.; Tischler, D. N-terminus determines activity
497 and specificity of styrene monooxygenase reductases. *BBA Proteins Proteom.* **2017**, *1865*, 1770-1780, DOI:
498 10.1016/j.bbapap.2017.09.004.
- 499 24. Otto, K.; Hofstetter, K.; Röthlisberger, M.; Witholt, B.; Schmid, A. Biochemical characterization of StyAB
500 from *Pseudomonas* sp. strain VLB120 as a two-component flavin-diffusible monooxygenase. *J. Bacteriol.* **2004**,
501 *186*, 5292-5302, DOI: 10.1128/JB.186.16.5292-5302.2004.
- 502 25. Watanabe, Y.; Numata, T.; Oae, S. Mild and facile preparation of sulfoxides from sulfides using titanium(III)
503 chloride/hydrogen peroxide. *Synthesis* **1981**, *1981*, 204-206, DOI: 10.1055/s-1981-29384.
- 504 26. Anderson, J.L.; Ding, J.; McCulla, R.D.; Jenks, W.S.; Armstrong, D.W. Separation of racemic sulfoxides and
505 sulfinate esters on four derivatized cyclodextrin chiral stationary phases using capillary gas
506 chromatography. *J. Chrom. A* **2002**, *946*, 197-208, DOI: 10.1016/S0021-9673(01)01526-6.
- 507 27. van den Heuvel, R.H.H.; Westphal, A.H.; Heck, A.J.R.; Walsh, M.A.; Rovida, S.; van Berkel, W.J.H.; Mattevi,
508 A. Structural studies on flavin reductase PheA2 reveal binding of NAD in an unusual folded conformation
509 and support novel mechanism of action. *J. Biol. Chem.* **2004**, *279*, 12860-12867, DOI: 10.1074/jbc.M313765200.
- 510 28. Kumar, S.; Stecher, G.; Tamura, K. MEGA7: Molecular Evolutionary Genetics Analysis Version 7.0 for
511 bigger datasets. *Mol. Biol. Evol.* **2016**, *33*, 1870-1874, DOI: 10.1093/molbev/msw054.
- 512 29. Robert, X.; Gouet, P. Deciphering key features in protein structures with the new ENDscript server. *Nucleic
513 Acids Res.* **2014**, *42*, W320-W324, DOI: 10.1093/nar/gku316.
- 514 30. Sali, A.; Blundell, T.L. Comparative protein modelling by satisfaction of spatial restraints. *J. Mol. Biol.* **1993**,
515 *234*, 779-815, DOI: 10.1006/jmbi.1993.1626.
- 516 31. Sambrook, J.; Russell, D.W. In *Molecular cloning: A laboratory manual*, Vol. 3, Cold Spring Harbor Laboratory
517 Press, Cold Spring Harbor, N.Y., 2001; ISBN 978-0879695767.
- 518 32. Miller, J.H. In *Experiments in Molecular Biology*, Cold Spring Harbor Laboratory Press, Cold Spring Harbor,
519 N.Y., 1972; pp. 431-433, ISBN 978-0879691066.
- 520 33. Puigbo, P.; Guzman, E.; Romeu, A.; Garcia-Vallve, S. OPTIMIZER: a web server for optimizing the codon
521 usage of DNA sequences. *Nucleic Acids Res.* **2007**, *35*, W126-W131, DOI: 10.1093/nar/gkm219.
- 522 34. Qi, J.; Schlömann, M.; Tischler, D. Biochemical characterization of an azoreductase from *Rhodococcus opacus*
523 1CP possessing methyl red degradation ability. *J. Mol. Catal., B Enzym.* **2016**, *130*, 9-17, DOI:
524 10.1016/j.molcatb.2016.04.012.
- 525 35. Bradford, M.M. A rapid and sensitive method for the quantitation of microgram quantities of protein
526 utilizing the principle of protein-dye binding. *Anal. Biochem.* **1976**, *72*, 248-254, DOI: 10.1016/0003-
527 2697(76)90527-3.

528 **Sample Availability:** Samples of the compounds or plasmids are available from the authors.